Journal of Cleaner Production 100 (2015) 333–343

Contents lists available at ScienceDirect

Journal of Cleaner Production

journal homepage: www.elsevier.com/locate/jclepro

Factorial experimental design for Remazol Yellow dye sorption using apple pulp/apple pulp carbon–titanium dioxide co-sorbent

Nurgul Ozbay*, Adife Seyda Yargic

Chemical and Process Engineering Department, Engineering Faculty, Gulumbe Campus, Bilecik Seyh Edebali University, 11210 Bilecik, Turkey

ARTICLE INFO

Article history:
Received 11 November 2014
Received in revised form
16 March 2015
Accepted 17 March 2015
Available online 25 March 2015

Keywords:
Apple pulp
Full factorial experimental design
Remazol Yellow
Sorption
TiO_2

ABSTRACT

Dye containing effluents can cause severe organic and color pollution in the water environment, thus removal of reactive dyes by sorption is an important circumstance. The aim of this study was to identify the operating conditions which influence Remazol Yellow dye sorption from aqueous solutions. There are limited numbers of literature studies about Remazol Yellow dye sorption. Despite that the sorption of Remazol Yellow dye by co-sorbent system and optimization of such process have not yet been studied. Thus, apple pulp and carbonized apple pulp at 550 °C were used as sorbents, also apple pulp–titanium dioxide and apple pulp carbon–titanium dioxide mixtures were used as co-sorbents. Elemental analysis, X-ray fluorescence spectroscopy, scanning electron microscopy, zeta potential, particle size distribution, and Fourier transform infrared spectroscopy analysis were conducted to analyze apple pulp and apple pulp carbon. The effects of pH, initial dye concentration and contact time were investigated by 3^3 full factorial experimental design method and analysis of variance statistical approach to optimize the operating conditions. The maximum percentage dye removal was obtained as 86.97% (sorbent type = apple pulp–titanium dioxide, pH = 2, initial dye concentration = 10 mg/L and contact time = 120 min). pH, initial dye concentration and contact time were found as significant within a 95% confidence level for all type of sorbents. Equilibrium isotherm data were fitted to Langmuir and Freundlich equations and the Langmuir model showed the best fit with equilibrium isotherm data. Furthermore, pseudo-first and second-order kinetic models were also used to analyze sorption kinetics. Since apple pulp was low-cost and easily available material, and also application of co-sorbent was influential for dye sorption; it could be successfully applied for the removal of Remazol Yellow dye from aqueous solutions.

1. Introduction

Textile, paints, paper, plastic, tanning, leather, food processing, and pharmaceuticals manufacturing to coloring products discharge synthetic dyes as serious organic pollutants into the environment (Zolgharnein et al., 2014). Dyes are stable, recalcitrant, colorant, and even potentially carcinogenic and toxic, so their release into the environment poses serious environmental, aesthetical and health problems. Therefore, industrial dye containing effluents are an increasingly major concern and need to be effectively treated before being discharged into the environment in order to prevent these potential hazards (Elkady et al., 2011).

Recently, several techniques have been performed for the removal of textile dyes from wastewater, including chemical oxidation (Khorramfar et al., 2011), anaerobic treatment (Kokabian et al., 2013), adsorption (Özbay et al., 2013), biosorption (Abdallah and Taha, 2012), coagulation (Wei et al., 2012), membrane filtration (Barredo-Damas et al., 2012) and photocatalysis (Yuan et al., 2012). High removal efficiency, simplicity and easy operation of textile dyes containing wastewater are the advantages of adsorption method (Yola et al., 2014). The activated carbon has been regarded as an excellent adsorbent, but it was sometimes treated as one-off adsorbent due to troublesome and high-cost regeneration. So it is necessary to find more efficient and cheaper alternate adsorbent (Wang et al., 2014). A number of researchers have investigated different low-cost adsorbents such as Ball clay (Auta and Hameed, 2012), natural Fouchana and Tabarka clays (Abidi

Abbreviations: ANOVA, analysis of variance; AOPs, advanced oxidation processes; AP, apple pulp; APC, apple pulp carbon; ATR, attenuated total reflectance technique; FT-IR, Fourier transform infrared spectroscopy; *RY*, Remazol Yellow; SEM, scanning electron microscope; XRF, X-ray fluorescence spectrometer.

* Corresponding author. Tel.: +90 228 2141220; fax: +90 228 2141222.
E-mail address: nurgul.ozbay@bilecik.edu.tr (N. Ozbay).

http://dx.doi.org/10.1016/j.jclepro.2015.03.050
0959-6526/

et al., 2015), bagasse pith (Allen et al., 1994), fly ash (Kara et al., 2007), fertilizer waste (Jain et al., 2003), coconut mesocarp (Vieira et al., 2009), blast furnaces slag (Ramakrishna and Viraraghavan, 1997), jujuba seeds (Reddy et al., 2012), sugar beet pulp (Aksu and Isoglu, 2006), wheat husk (Gupta et al., 2007), silkworm pupa (Noroozi et al., 2007), eggshell (Elkady et al., 2011), hen feathers (Mittal et al., 2007), polymer–clay nanocomposites (Zhou et al., 2014), wild olive cores (Kaouah et al., 2013), *Jatropha curcas* pods (Sathishkumar et al., 2012) and tomato waste (Yargıç et al., 2015).

The recent trend in treatment of organics and dyes has shifted from phase transfer to destruction of pollutants, i.e., advanced oxidation processes (AOPs). Among AOPs, top priority goes to photocatalytic degradation (Farzana and Meenakshi, 2014). With the development of nano-technology, nanostructured TiO_2 is found to have good adsorptive and photocatalytic property simultaneously for dye removal. The adsorbed dyes can be degraded completely by TiO_2 adsorbents in the subsequent photocatalytic process and thus cost of regeneration is low (Wang et al., 2014). Nowadays, some studies have been achieved to evaluate the efficiency of photocatalysts using TiO_2 with activated carbon as co-catalyst. The comparison of the adsorption and photodegradation methods for the removal of basic violet 10 dye by using activated carbon prepared from rice husk (RC) and RC + TiO_2 mixture (Ravichandran et al., 2013). Liu et al. deposited TiO_2 thin films on granular activated carbon by a dip-coating method and used TiO_2/AC for phenol degradation (Liu et al., 2007). TiO_2 photocatalysts deposited on activated carbon (TiO_2/AC) were prepared by dip-hydrothermal and their photocatalytic activity was evaluated by degradation of methyl orange (Wang et al., 2009). A synergetic effect has been observed by using powdered TiO_2 and powdered activated carbon in the photocatalytic degradation of organic pollutants. This synergetic effect has been ascribed to the presence of a common contact interface spontaneously created between both solids (Farzana and Meenakshi, 2014).

Apples constitute one of the most abundant fruits, with a world production of 76.4 million metric tons (Mt) in 2012 (Food and Agriculture Organization of the United Nations, 2014). Apple is one of the soft-core fruit and has very significant role for Turkish trade since Turkey is in the third place for apple production (2.550 thousand tons in a year) in the world (Depci et al., 2012). Although apples are especially consumed directly as a fruit, about 12% of the production is destined to the manufacture of apple juice and cider. In turn, pressing apples generates the solid residue (apple pulp) which represents more than 12 wt.% of the fruit. Therefore, taking an intermediate value of 60 Mt for the yearly world production, about 0.84 Mt of apple pulp are generated yearly worldwide. Although it is not as polluting as other vegetable by-products from the food industry, apple pulp is a useless material that is often spilled in a non-controlled way (Suárez-Garcıa et al., 2001).

The aim of this study was to investigate the usability of apple pulp/apple pulp carbon–TiO_2 co-sorbents to remove Remazol Yellow dye from aqueous solutions. Thus, the apple pulp (*AP*) was used as potential alternative precursor to obtained carbonaceous material (*APC*). Analysis of variance (ANOVA) statistical approach and 3^3 full factorial design were used to evaluate the significance of three experimental factors (pH, initial dye concentration and contact time) concerning the dye removal efficiency. Besides this, the kinetic study was carried out by pseudo-first and pseudo-second order kinetic models. Equilibrium isotherm data were fitted to Langmuir and Freundlich equations; constants of isotherm equations were determined. To our knowledge, previous studies have not yet reported the optimization of dye sorption conditions when biomass and TiO_2 are used as co-sorbent. Nanoparticles have high sorption capacity, the operation is simple, and the sorption process is rapid. Apple pulp/apple pulp carbon–TiO_2 co-sorbents would be expected to present copious benefits from an environmental point of view such as, sustainable availability, increasing the sorption efficiency due to the synergistic photocatalysis-sorption hybrid system and easy storage. Eventually, another goal of this study was to complete the shortcomings in the literature by using biomass-nanoparticle mixtures in sorption.

Table 1
Factors and their levels studied in full factorial design.

Factors	Levels		
	1	2	3
pH *(A)*	2	6	10
Initial concentration, mg/L *(B)*	10	50	100
Contact time, min *(C)*	40	80	120

Table 2
The results for ultimate and proximate analyses.

Ultimate analysis		
Component (%)	AP	APC
C	46.54	69.38
N	1.08	1.13
H	6.91	2.53
O[a]	45.48	26.97
HHV (MJ/kg)	25.70	27.11
Proximate analysis of *AP*		
		wt.%
Preliminary analysis		
Moisture		8.84
Ash		9.2
Volatile		76.77
Fixed carbon[a]		5.19
Structural analysis		
Holocellulose		48.99
Hemicellulose		18.66
Extractive material		12.51
Lignin		29.29
Cellulose[a]		30.33

[a] Estimated by difference.

2. Material and methods

The decision of sorbent types and modification of them are essential to remove dye; therefore characteristics of sorbent should be identified and optimization of experimental conditions should be done carefully.

Table 3
Chemical composition of *AP*.

Component	Concentration (%)
Mg	0.097
P	0.509
S	0.275
K	1.138
Ca	1.515
Mn	0.026
Fe	0.157
Cu	0.030
Zn	0.016
Rb	0.007
Sr	0.009

2.1. Preparation of sorbents and aqueous dye solutions

Apple pulp obtained from a fruit juice factory in Bursa (Turkey) was air-dried, crushed and sieved to obtain mean sizes. Apple pulp was carbonized at 550 °C with a heating rate of 10 °C/min to produce carbonaceous product. Apple pulp (*AP*) and apple pulp carbon (*APC*) were stored in plastic bottles for further use. Nano-TiO_2 (98+%, anatase powder) was obtained from Acros, and calcined at 550 °C for 5 h with a heating rate of 5 °C/min. *AP*, *APC*, *AP*–TiO_2 mixture, *APC*–TiO_2 mixture were used as sorbents. To prepare the sorbents, TiO_2 nanoparticle was mixed with *AP* or *APC* with a ratio of 3:1.

Reactive textile dye Remazol Yellow (*RY*, color index: Reactive Yellow 15) was used without purification. Dye solutions were prepared using distilled water to prevent and minimize possible interferences. Stock solution of dye (1000 ppm) was prepared by dissolving 1.0 g of *RY* dye in 1000 mL of distilled water. Different working concentrations (10–100 mg/L) were arranged by diluting the standard solution of dye. The pH of the solution was adjusted by adding 0.1 M NaOH or 0.1 M HCl, and it was monitored by a digital pH meter Thermo Scientific Orion 3 Star.

2.2. Characterization and analysis

Different characterization techniques were used to identify the properties of sorbents. The ultimate analysis of *AP* and *APC* was performed by Elemental Analyzer (Leco CNH628 S628) to find carbon, hydrogen, nitrogen and oxygen contents of materials by using helium, dry air and oxygen gases. The complete combustion of all organic samples was carried out by operating Elemental Analyzer's furnace at 950 °C. Structure and preliminary analysis were carried out to complete the proximate analysis of *AP*. Functional groups of *AP* and *APC* were estimated by Fourier transform infrared (FT-IR) spectroscopy (Perkin Elmer Spectrum 100) in the range of 400–4000 cm^{-1}. The FT-IR spectrums of AP and APC were obtained using the ATR technique (with a diamond protected Attenuated Total Reflectance crystal unit) with a resolution of 4 cm^{-1} after 100 scans. Surface morphologies of *AP* and *APC* were observed by employing a scanning electron microscope (Zeiss Supra VP 40) with an accelerating voltage of 5 kV. The samples were sputter-coated with platinum (Qourum Q 150 R ES DC Sputter). The chemical analysis of apple pulp was determined by using X-ray fluorescence (XRF) spectrometer (Empyrean Panalytical Axios Max Minerals). The zero surface charge characteristics of *AP* and *APC* were determined by the solid addition method (Vieira et al., 2009). The solutions (20 mL) with pH varying of 1–10 were transferred to a series of 100 mL conical flask. The pH_i values of each solution were adjusted by adding either 0.1 N HCl or NaOH and were measured. *AP* and *APC* were added to each flask; the suspensions were then manually shaken and were analyzed by Malvern Zeta Sizer Nano Series Nano-ZS. Zeta potential (mV) of particles was plotted against pH and the point of intersection of the resulting curve with absisca, at which pH 0, gave pH_{ZPC}. Finally, particle size analysis of *AP* and *APC* were performed by using Malvern Mastersizer Hydro 2000S.

2.3. Batch sorption studies

For the decolorization of Remazol Yellow dye solution, batch studies were achieved at room temperature to study the effect of parameters such as pH, contact time and initial dye concentration. Batch sorption experiments were conducted in a set of conical flasks containing 50 mL dye solution of different operating conditions with 0.3 g sorbent. The suspensions were then filtered and dye concentrations in the supernatant solutions were measured. Standard curves were developed at λ_{max}, 422 nm for Remazol Yellow dye, through the measurement of the dye solution absorbance by UV/Visible Spectrophotometer (V-530 Jasco UV/VIS).

The following equations were utilized for determining the uptake capacity of dye (q_e) from aqueous solutions and the dye removal efficiency (η) (Ahmad and Rahman, 2011):

$$q_e = (C_0 - C_e)V/W \quad (1)$$

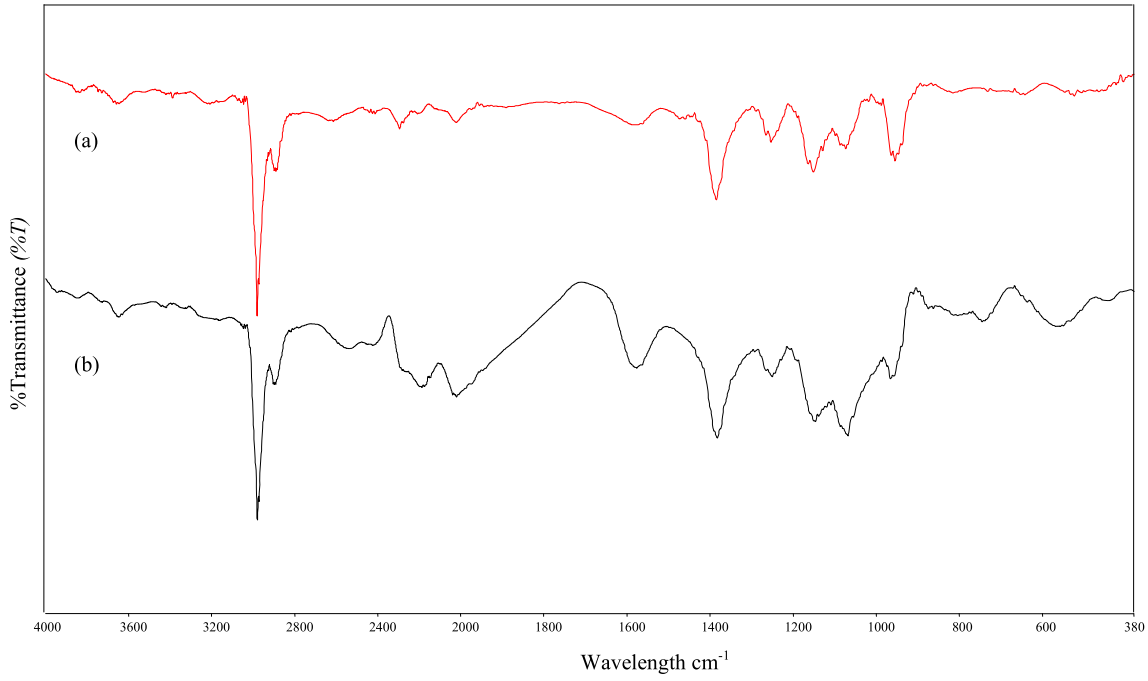

Fig. 1. FT-IR spectrums of (a) *AP*, (b) *APC* obtained at 550 °C.

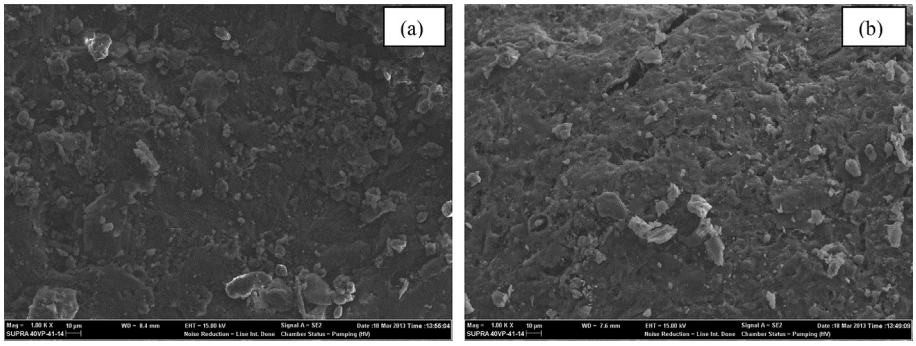

Fig. 2. SEM images of (a) *AP* and (b) *APC*.

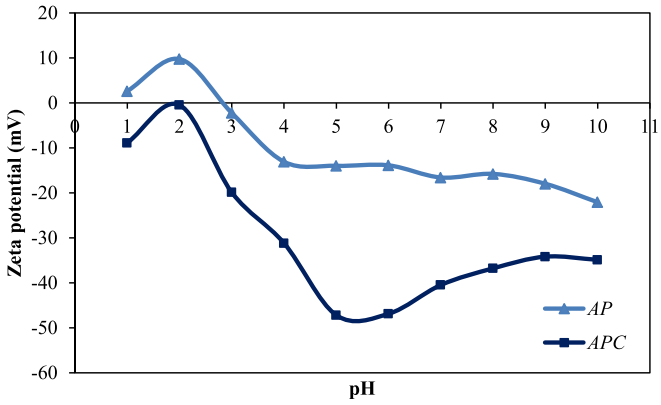

Fig. 3. Determination of the point of zero charge of *AP* and *APC*.

Table 4
Experimental design matrix of *RY* sorption.

Runs	Factors			Removal efficiency (%)			
	A	*B*	*C*	*AP*	*AP*–TiO_2	*APC*	*APC*–TiO_2
1	1	1	1	46.85	83.47	31.06	75.54
2	1	1	2	48.1	86.18	34.39	78.77
3	1	1	3	49.34	86.97	38.53	79.4
4	1	2	1	31.3	74.48	15.62	46
5	1	2	2	37.16	82.11	18.07	47.24
6	1	2	3	43.17	84.07	23.71	63.78
7	1	3	1	25.92	47.67	11.36	17.57
8	1	3	2	26.6	56.91	10.28	18.42
9	1	3	3	31.59	66.48	12.73	41.43
10	2	1	1	23.11	60.74	12.48	13.68
11	2	1	2	37.64	65.53	16.16	18.08
12	2	1	3	47.06	73.88	16.64	26.48
13	2	2	1	27.33	39.77	1.11	11.06
14	2	2	2	34.76	46.85	2.04	15.66
15	2	2	3	43.21	54.25	6.01	20.78
16	2	3	1	10.1	28.16	3.84	10.31
17	2	3	2	14.38	34.93	5.83	11.63
18	2	3	3	19.05	37.31	10.87	18.35
19	3	1	1	24.8	48.59	1.60	7.96
20	3	1	2	27.54	56.77	3.53	9.25
21	3	1	3	31.77	72.31	5.17	15.61
22	3	2	1	12.84	39.64	2.08	4.4
23	3	2	2	15.09	42.84	3.94	6.35
24	3	2	3	18.27	49.68	5.07	10.75
25	3	3	1	5.5	13.61	3.46	2.3
26	3	3	2	7.71	25.58	3.72	4.86
27	3	3	3	8.74	31.73	4.07	6.84

$$\eta = [(C_0 - C_e)/C_0]100 \quad (2)$$

where q_e is the amount of dye sorbed on the sorbent (mg/g), C_0 and C_e (mg/L) are the liquid phase concentrations of dye at initial and equilibrium, respectively. V (L) is the volume of dye solution and W (g) is the amount of the sorbent used.

2.4. Statistical design of experiments

The factorial design helps to develop a statistical model of a reaction by performing the minimum number of well-chosen experiments and to determine the optimal values of process parameters. Factorial design is an empirical modeling technique used to evaluate the relationship between experimental variables and corresponding responses (Prasad and Srivastava, 2009). Since the three factors pH, initial dye concentration, and contact time were varied at three levels, the factorial of the type 3^3 was applied. The factors and their respective levels were presented in Table 1. The parameters were pH (2, 6 and 10), initial dye concentrations (10, 50 and 100 mg/L) and contact time (40, 80 and 120 min) which were chosen according to common literature studies.

2.5. Equilibrium and kinetic modeling

It is important to establish the most appropriate correlation for the equilibrium curves (Leechart et al., 2009) to optimize the design of sorption systems for removal of dye. The experimental data of *RY* dye was analyzed using linear Langmuir and Freundlich isotherm models to investigate the equilibrium characteristics of sorption. Linear regression is generally used to find which isotherm is best fitted, and also the correlation coefficients of R^2 are evaluated to compare the practicality of isotherm equation.

The Langmuir isotherm in Eq. (3), assumes monolayer adsorption onto a surface containing a finite number of identical

Table 5
Analysis of variance (ANOVA) for *AP*.

Source	DF	Seq SS	Adj SS	Adj MS	F	P
A	2	1966.91	1966.91	983.46	128.95	0.000
B	2	1965.15	1965.15	982.57	128.84	0.000
C	2	396.28	396.28	198.14	25.98	0.000
*A***B*	4	178.02	178.02	44.50	5.84	0.017
*A***C*	4	109.88	109.88	27.47	3.60	0.058
*B***C*	4	28.07	28.07	7.02	0.92	0.497
Error	8	61.01	61.01	7.63		
Total	26	4705.32				

$S = 2.76159$ R-Sq = 98.70% R-Sq(adj) = 95.79%.

adsorption sites. The Freundlich isotherm in Eq. (4), assumes heterogeneous surface energies on the adsorbent surface, in which the energy term in Langmuir equation varies as a function of the surface coverage (Özbay et al., 2013).

$$C_e/q_e = 1/(K_L q_m) + C_e/q_m \quad (3)$$

$$\log q_e = \log K_F + (1/n)\log C_e \quad (4)$$

where q_m (mg/g) and K_L (L/mg) are Langmuir constants related to maximum sorption capacity and rate of sorption, respectively. Also, q_e (mg/g) is the amount of dye sorbed per unit weight of sorbent; C_e (mg/L) is the concentration of the dye solution at equilibrium. K_F (mg/g(L/mg)$^{1/n}$) and n are the Freundlich sorption constant and heterogeneity factor, respectively. K_F is related to the bonding energy and $1/n$ value is related to the sorption intensity. The intercept K_F and the slope $1/n$ are obtained by plotting $\ln q_e$ versus $\ln C_e$.

Pseudo-first order (Eq. (5)) and pseudo-second order (Eq. (6)) kinetic models were tested to evaluate the possible mechanism of *RY* dye sorption process by using the data obtained from sorption kinetic experiments. When sorption is preceded by diffusion through a boundary, the kinetics in most systems follow pseudo-first order equation (Foo and Hameed, 2011). The pseudo-second order model estimates the behavior over the whole range adsorption and this model is also based on the adsorption capacity of the solid phase. The pseudo-second order model has a supposition that the sorption process involves chemisorption mechanism (Özbay et al., 2013).

$$\log(q_e - q_t) = \log q_e - (k_1 t)/2.303 \quad (5)$$

$$t/q_t = 1\Big/\left(k_2 q_e^2\right) + (1/q_e)t \quad (6)$$

where k_1 is the rate constant of pseudo-first order sorption (min^{-1}), k_2 is the rate constant of pseudo-second order sorption (g/mg min), t is the contact time (min), q_e and q_t (mg/g) are the amounts of *RY* sorbed at equilibrium and at time t (min) (Özbay et al., 2013).

3. Results and discussion

In this part, characteristics of apple pulp and apple pulp carbon, statistical results of dye sorption, parameters of kinetic and isotherm studies were investigated.

3.1. Characterization of AP and APC

The results for ultimate and proximate analyses *AP* and ultimate analysis of *APC* were presented in Table 2. After carbonization process, the carbon content and calorific value increased significantly whereas the oxygen content decreased in the sample; which indicated that *APC* was more carbonaceous material than *AP*.

Table 6
Analysis of variance (ANOVA) for *AP*–TiO_2.

Source	DF	Seq SS	Adj SS	Adj MS	F	P
A	2	5106.72	5106.72	2553.36	175.68	0.000
B	2	4786.17	4786.17	2393.09	164.65	0.000
C	2	807.47	807.47	403.74	27.78	0.000
*A*B*	4	184.76	184.76	46.19	3.18	0.077
*A*C*	4	40.49	40.49	10.12	0.70	0.615
*B*C*	4	40.49	40.49	5.48	0.38	0.819
Error	8	116.27	116.27	14.53		
Total	26	11063.81				

$S = 3.81236$ R-Sq = 98.95% R-Sq(adj) = 96.58%.

Table 7
Analysis of variance (ANOVA) for *APC*.

Source	DF	Seq SS	Adj SS	Adj MS	F	P
A	2	1499.73	1499.73	749.86	315.91	0.000
B	2	602.19	602.19	301.09	126.85	0.000
C	2	107.39	107.39	53.69	22.62	0.000
*A*B*	4	494.80	494.80	123.70	52.11	0.000
*A*C*	4	17.24	17.24	4.31	1.82	0.219
*B*C*	4	9.66	9.66	2.42	1.02	0.453
Error	8	18.99	18.99	2.37		
Total	26	2750.00				

$S = 1.54068$ R-Sq = 99.31% R-Sq(adj) = 97.76%.

Table 8
Analysis of variance (ANOVA) for *APC*–TiO_2.

Source	DF	Seq SS	Adj SS	Adj MS	F	P
A	2	9976.73	9976.73	4988.36	273.99	0.000
B	2	2084.04	2084.04	1042.02	57.23	0.000
C	2	544.44	544.44	272.22	14.95	0.002
*A*B*	4	2105.67	2105.67	526.42	28.91	0.000
*A*C*	4	87.96	87.96	21.99	1.21	0.379
*B*C*	4	26.87	26.87	6.72	0.37	0.825
Error	8	145.65	145.65	18.21		
Total	26	14971.34				

$S = 4.26687$ R-Sq = 99.03% R-Sq(adj) = 96.84%.

According to XRF results of *AP* given in Table 3, main constituents were found as calcium and potassium with concentration (%) of 1.515 and 1.138. According to particle size analysis, main particle size distribution of *AP* and *APC* were found as 149.3 nm and 106.9 nm, respectively.

The FT-IR spectrum was conducted to determine the functional groups of the materials. The FT-IR analysis of *AP* and *APC* were presented in Fig. 1(a) and (b), respectively. The main functional groups were O–H stretching vibration of hydroxyl functional groups including hydrogen bonding which was detected at bandwidths of 3300–3200 cm^{-1} (Özbay et al., 2013). Other major peaks detected between 2970 and 2890 cm^{-1} were attributed to symmetric and asymmetric C–H stretching of aliphatic methyl and methylene. Peaks observed at 1582 cm^{-1} for both *AP* and *APC* were assigned to the aromatic C=C ring stretch. C–H stretching bands of aliphatic CH_3 groups were appeared at 1460 cm^{-1} and 1382 cm^{-1}. Small band at 1250 cm^{-1} was assigned to CH=CH stretching and also small bands ranging from 1100 to 1000 cm^{-1} were assigned to C–O stretching vibrations of lignin (Cardoso et al., 2011). Peaks located at bandwidths of 700–500 cm^{-1} could be assigned to C–H out-of-plane bending in benzene derivatives. The C–H out-of-plane bending in benzene derivatives was commonly found on the surface of various activated carbons (Ahmad and Rahman, 2011).

Scanning electron microscopy (SEM) technique was used to observe the surface physical morphology of *AP* and *APC*. SEM images of *AP* and *APC* sorbents 1000× magnification were given in Fig. 2. According to micrographs, it could be seen that the surface of *AP* (Fig. 2(a)) was irregular without any pores except for some occasional cracks. Surface of *APC* contained more pores than AP surface because of carbonization process.

Zeta potential analysis results of *AP* and *APC* were given in Fig. 3. The zeta potential of particles was between approximately +10 mV and −50 mV. The surface charges of *AP* and *APC* around pH 3 and 2 were found as zero, respectively. *RY* removal was higher around pH 2 as seen in the main effects plots (Fig. 6). Higher *RY* dye removal under acidic conditions was most likely due to the excessive positive charge on dye anion *RY* for the sorption sites. Reddy et al. reported a similar behavior for Congo red dye removal by jujuba seeds (Reddy et al., 2012).

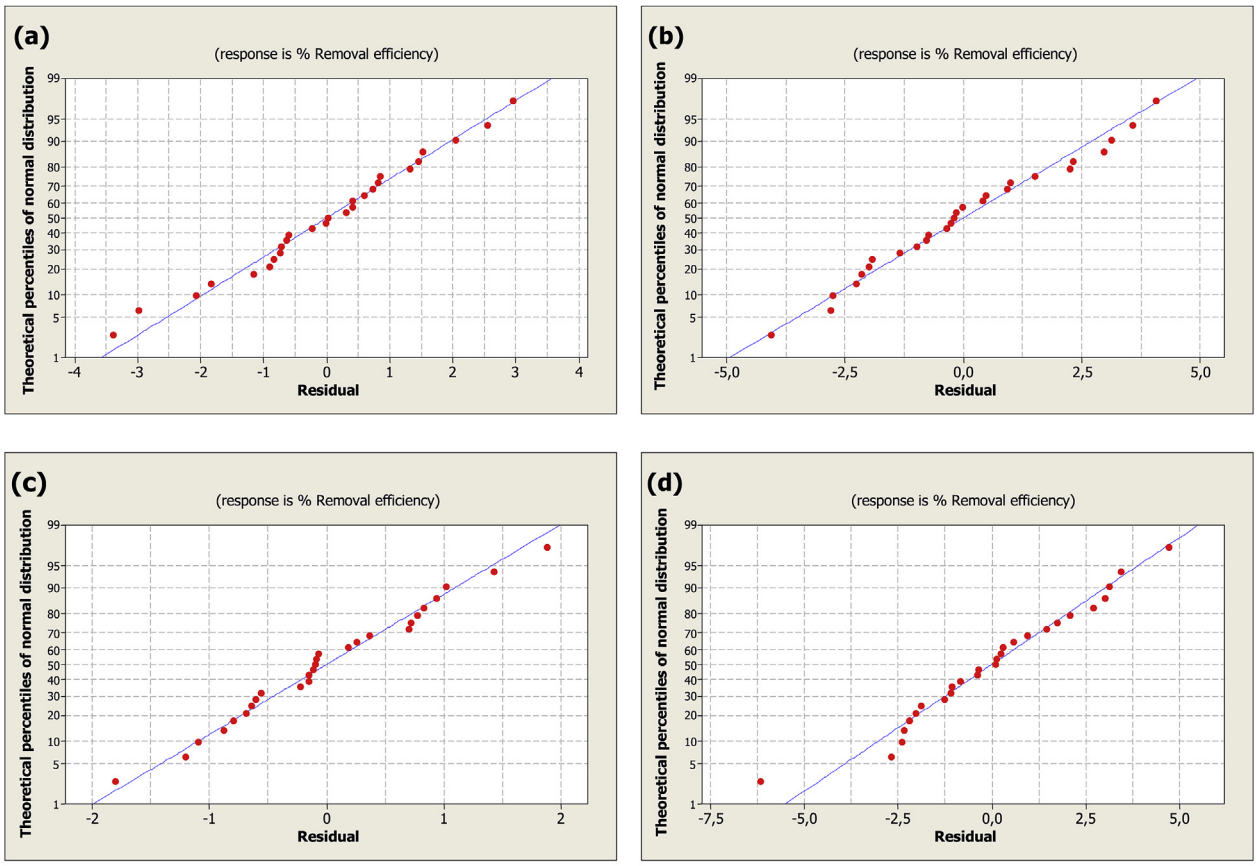

Fig. 4. Normal probability plot of residuals for % removal efficiency of (a) *AP*, (b) *AP*–TiO_2, (c) *APC*, and (d) *APC*–TiO_2.

3.2. Statistical analysis

Full factorial design (3^3) was used to optimize the parameters which affect the sorption experiments. The results of the experimental design were analyzed using MINITAB 14 statistical software to evaluate the effects as well as the statistical parameters and the statistical plots (residuals versus the fitted values, normal probability of residuals, main effects, and interaction plots). The coded values of variables with the responses (% removal efficiency) were illustrated in Table 4. The studied variables were pH of solution (2, 6 and 10), initial dye concentration (10, 50 and 100 mg/L) and contact time (40, 80 and 120 min). The number of experiments was given by $a^k = 3^3 = 27$ where a and k were the number of levels and the number of factors (Kavak, 2009). The interactions between independent factors were determined with analysis of variance (ANOVA) and the main effects of dye sorption were identified based on the *P*-value with >95% of confidence level.

Following codified equation was used to explain the 3^3 factorial designs of *RY* removal by sorption:

$$\begin{aligned} Y = {} & Xo + A[1] + A[2] + B[1] + B[2] + C[1] + C[2] + A[1]B[1] \\ & + A[2]B[1] + A[1]B[2] + A[2]B[2] + A[1]C[1] + A[2]C[1] \\ & + A[1]C[2] + A[2]C[2] + B[1]C[1] + B[2]C[1] + B[1]C[2] \\ & + B[2]C[2] + A[1]B[1]C[1] + A[2]B[1]C[1] + A[1]B[2]C[1] \\ & + A[2]B[2]C[1] + A[1]B[1]C[2] + A[2]B[1]C[2] + A[1]B[2]C[2] \\ & + A[2]B[2]C[2] \end{aligned} \quad (7)$$

where *Y* is the predicted response (% removal efficiency), X_0 represents the global mean, *A* is the solution pH, *B* is the initial dye concentration (mg/L) and *C* is the contact time (min).

3.2.1. Analysis of variance (ANOVA)

There are several important concerns with the conventional approach of changing one or two variables in a run. It may take several rounds of experiments to find the optimum point. In cases where variables must be changed in large steps the optimum may not be found at all. Factorial design consists of different treatments of all possible combinations of several levels of factors. It reveals the effect of interaction of process variables and improves process optimization. Moreover, the relative importance of all the factors can be evaluated simultaneously with less number of treatments (Safa and Bhatti, 2011). Analysis of variance is a statistical method that partitions the total variation into its component parts each of which is associated with a different source of variation (Özbay et al., 2013). The interaction effects are easily estimated and tested by using the usual ANOVA. The ANOVA results of *RY* were shown in Tables 5–8. The sum of the squares used to estimate factors affect and Fisher's F-ratios and *P*-values were also represented.

ANOVA predicted that all of the main factors (solution pH, initial dye concentration and contact time) were highly significant ($P < 0.05$) and the model was applicable very well for all type of sorbents. The interactions (A^*B) were significant at a 5% of probability level except only *AP*–TiO_2 sorbent. Moreover, the fit models submitted square correlation coefficient (R^2) of 0.9870, 0.9895, 0.9931 and 0.9903 were in good agreement with the statistical model for *AP*, *AP*–TiO_2, *APC* and *APC*–TiO_2, respectively.

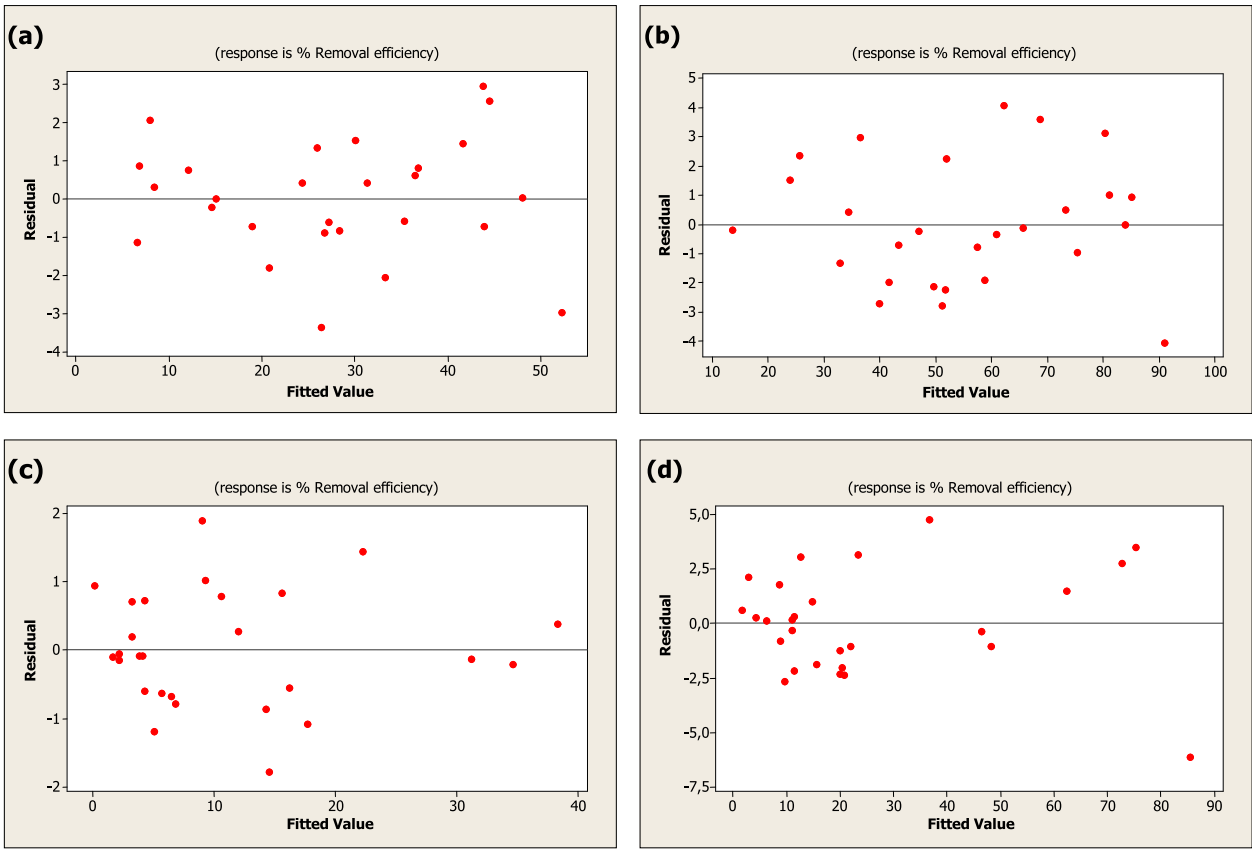

Fig. 5. RY dye removal vs. residual effects for (a) *AP*, (b) *AP*–TiO_2, (c) *APC*, and (d) *APC*–TiO_2.

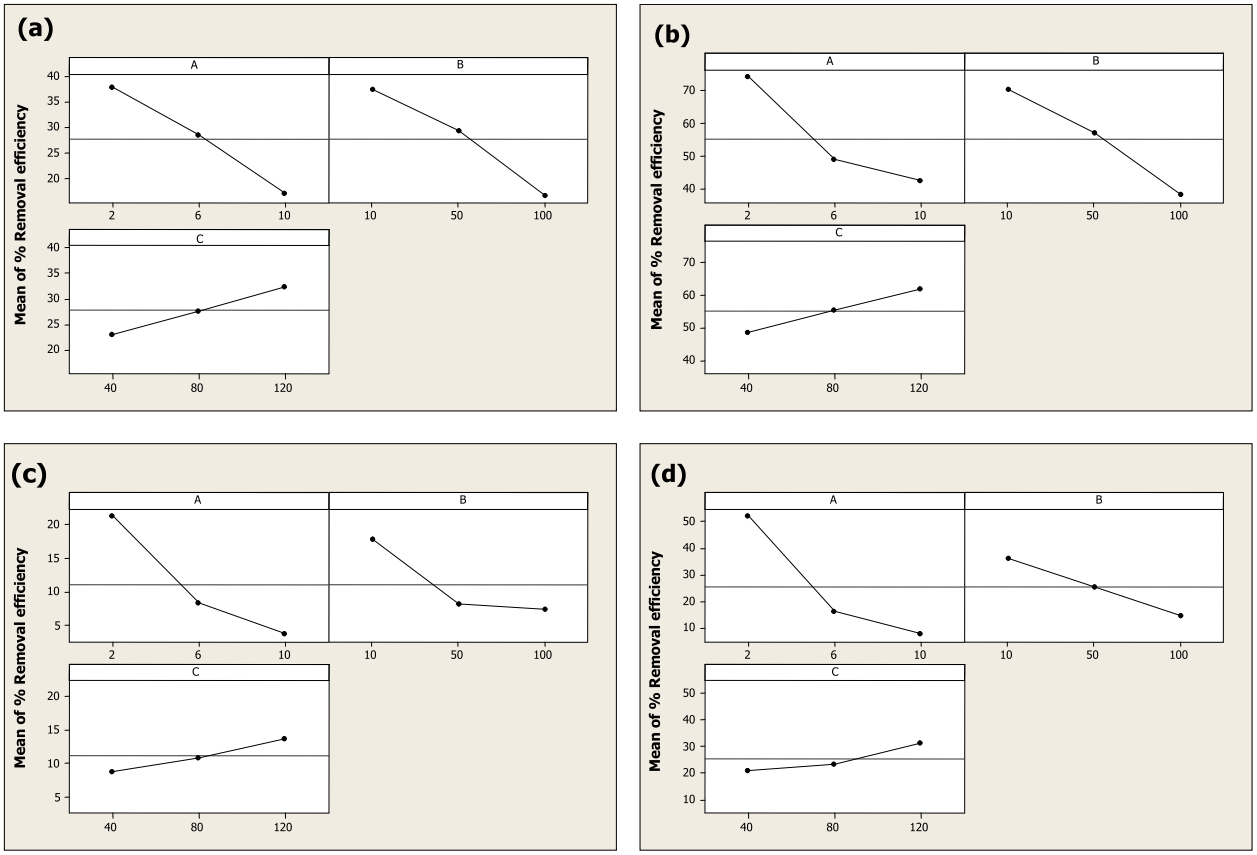

Fig. 6. Main effects plots of (a) *AP*, (b) *AP*–TiO_2, (c) *APC* and (d) *APC*–TiO_2 for the removal efficiency (%).

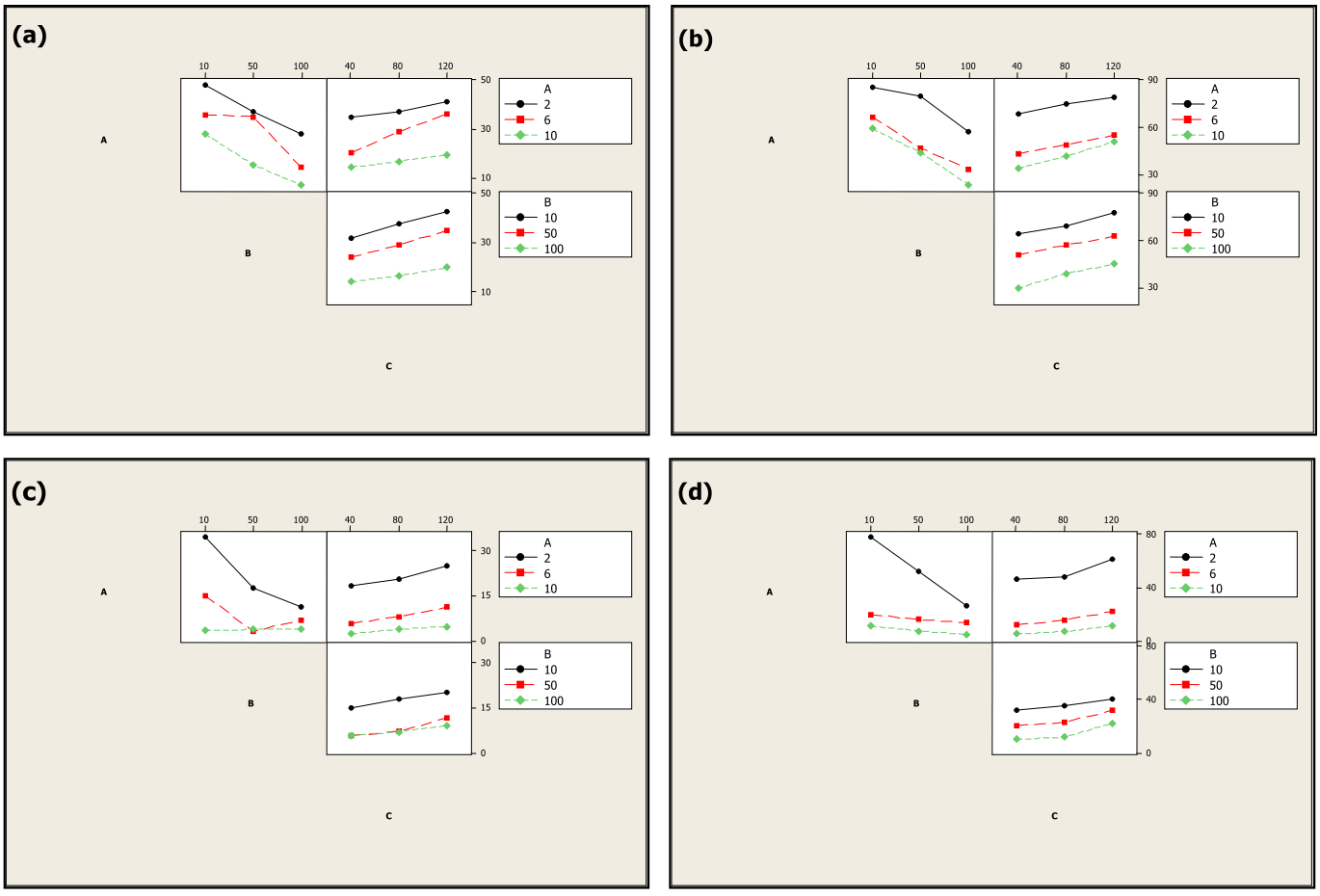

Fig. 7. Interaction effects plots of (a) *AP*, (b) *AP*–TiO_2, (c) *APC* and (d) *APC*–TiO_2 for the removal efficiency (%).

Table 9
Langmuir and Freundlich coefficients and regression correlation coefficients for sorption of *RY* dye.

Sorbent type	Langmuir isotherm			Freundlich isotherm		
	q_m (mg/g)	K_L (L/mg)	R^2	n	K_F	R^2
AP	9.09	0.0208	0.984	1.36	0.26	0.979
AP–TiO_2	14.71	0.0952	0.991	1.57	1.39	0.943
APC	2.54	0.0647	0.990	6,80	0.55	0.361
APC–TiO_2	8.13	0.0984	0.999	1.96	0.98	0.958

3.2.2. Normal probability plot of residuals

One of the most important assumptions for statistical analysis of data from experiments is that the data come from a normal distribution (Antony, 2003). If the points on the plot fall fairly close to a straight line, then the data are normally distributed (Srinivasan and Viraraghavan, 2010). Fig. 4 showed the normal probability plot of residual values. The residual values explain the difference between predicted values (model) and the observed values (experimental) (Safa and Bhatti, 2011). It could be seen that the experimental points were reasonably aligned suggesting normal distribution. All the points of normal probability plots

Table 10
The pseudo-first order and second order kinetic parameters for *RY* dye removal.

Sorbent type	Initial dye concentration (mg/L)	$q_{e,exp}$ (mg/g)	Pseudo-first order kinetic model			Pseudo-second order kinetic model		
			k_1 (min^{-1})	$q_{e,cal}$ (mg/g)	R^2	k_2 (g/(mg min))	$q_{e,cal}$ (mg/g)	R^2
AP	10	0.8223	0.0237	0.1271	0.9185	0.1755	0.8363	0.9996
	50	3.5975	0.0244	2.9356	0.9415	0.0092	4.1893	0.9928
	100	5.2650	0.0104	1.5663	0.7595	0.0226	5.0838	0.991
AP–TiO_2	10	1.4495	0.0313	0.1999	0.9683	0.2772	1.4764	1
	50	7.0058	0.0578	11.0458	0.9344	0.0137	7.6394	0.9999
	100	11.080	0.0283	11.2875	0.9028	0.0025	13.333	0.9881
APC	10	0.6423	0.0186	0.2754	0.9708	0.1150	0.6745	0.9983
	50	1.9762	0.0317	1.5173	0.9042	0.0260	1.9260	0.9953
	100	2.1232	0.0087	0.6248	0.7676	0.0590	2.0080	0.9917
APC–TiO_2	10	1.3234	0.0476	0.4960	0.9843	0.2122	1.3659	1
	50	5.3150	0.0020	1.6120	0.9534	0.0680	4.1476	0.9996
	100	6.9051	0.0064	5.5270	0.6696	0.0036	5.7306	0.7131

were found to fall in the range of +3.5 to −3.5, +5 to −5, +2 to −2 and +6 to −6 for *AP*, *AP*–TiO_2, *APC* and *APC*–TiO_2, respectively. Plot of percentage dye removal versus residual (Fig. 5) indicated the outliers if any. All the points were found to fall in the ranges of above mentioned, which suggested that the model indicated a minimal deviation at the fitted value from the observed value (Rathinam et al., 2011).

3.2.3. Main effects and interaction effects of the factors

The main effects of three factors (*A*, *B* and *C*) on % removal efficiency were presented in Fig. 6. The effect of a factor is the change in response produced by the change in level of factor. This is frequently called a main effect as it refers to the primary factor of interest in the experiment (Özbay et al., 2013). The statistical significance of a factor is directly related to the length of the vertical line. According to this notion, the larger the vertical line in main effect plots is the larger the change in % removal efficiency when it is changing from level 1 to level 3. The *ABC* effect, seemed insignificant compared to other effects, were neglected. The increase in the pH involved a striking decrease of *RY* uptake by sorbents. Surface area and active sites of sorbents may be saturated at higher concentrations, thus % removal efficiency decreased with raising the initial dye concentration (Kaouah et al., 2013). The characteristics of sorbents and their available sorption sites affected the time needed to reach the equilibrium. According to main effects plot, the removal efficiencies increased with increasing contact time.

Although the main effects gave a clear idea, the interaction between those two parameters would favor a better statement of the process. Fig. 7 illustrated the possible positive and negative two-variable interactions among the variables *A*, *B*, *C* for % removal efficiency. It was observed that the effect of pH was more noticeable when the initial dye concentration was low; however at higher initial dye concentration, effect of pH was not quite high. However, the effects of pH and initial dye concentration had similar trends, when contact time level was changed.

3.3. Kinetic and isotherm models

Adsorption isotherm is important for describing the adsorption behavior for solid–liquid system; another importance of adsorption study is to predict the order of adsorption. In this section, the results of sorption isotherms and kinetic models were presented.

3.3.1. Equilibrium adsorption isotherms

Langmuir and Freundlich isotherms of *RY* dye removal were performed using four sorbents at pH 2 for 120 min. Initial dye concentrations varied as 10, 50 and 100 mg/L; all constants and R^2 values obtained by both models were given in Table 9. The highest correlation coefficients (R^2 values) were obtained from Langmuir isotherm, thus the Langmuir model displayed better fit to the sorption data than the Freundlich model. This result indicated that the surface of sorbents for *RY* removal was made up of homogeneous sorption patches.

3.3.2. Adsorption kinetic models

Kinetic models describe the mechanism of sorption processes which in turn controls the equilibrium time and mass transfer of the adsorbates. *RY* dye with three different concentration (10, 50 and 100 mg/L) at pH = 2 was removed at different time intervals. Experimental data were investigated to have a good agreement between pseudo-first order and pseudo-second order models. The adsorption rate constants (k_1 and k_2), q_e and correlation coefficient (R^2) values were listed in Table 10. In relation to Table 10, all of the correlation coefficients, R^2 values for pseudo-second order kinetic model were higher than pseudo-first order kinetic model's and were close to unity. The data indicated that the calculated $q_{e,cal}$ values for the pseudo-second order kinetics were closer to the experimental $q_{e,exp}$ values compared to pseudo-first order values. Therefore, it could be concluded that *RY* sorption did not match with the pseudo-first order model. This result showed that a chemisorption mechanism most likely controlled the sorption.

4. Conclusions

The optimization of Remazol Yellow dye removal from aqueous solution by using *AP*, *APC*, *AP*–TiO_2 and *APC*–TiO_2 was achieved through 3^3 full factorial experimental design. The effects of pH (2–10), initial dye concentration (10–100 mg/L) and contact time (40–120 min) on % removal efficiency were identified.

- The increasing solution pH and initial dye concentration had negative effect, while increasing contact time had a positive effect on dye removal. Dye uptake was found as mostly pH-dependent and TiO_2 addition played an important role in % removal efficiency of dye.
- Maximum sorption of *RY* ion was obtained as 86.97% when apple pulp–TiO_2 co-sorbent used (pH = 2, initial dye concentration = 10 mg/L and contact time = 120 min).
- The surface charges of *AP* and *APC* around pH 3 and 2 were found as zero, respectively. This result supported that the dye sorption was more favorable at lower pH values.
- Based on the obtained substantial effect in ANOVA results, all of the main effects were significant. The interaction effect between pH and initial dye concentration was the most influencing interaction.
- The sorption equilibrium of Remazol Yellow was described by using the Langmuir and Freundlich isotherm models and the characteristic parameters for each isotherm were determined. The Langmuir model which referred homogeneous sorption was stated as the best fit for the sorption data.
- Pseudo first-order and pseudo second-order kinetic models were used to test the sorption kinetics. The data indicated that the sorption kinetics followed the pseudo-second order expression, so the sorption process was controlled by chemical sorption.

TiO_2–apple pulp mixture was performed as sorbent for the first time in the literature to remove dye. In order that TiO_2 nanoparticle was eco-friendly and also apple pulp was a potential low-cost and abundant material, utilization of co-sorbent could be an alternative, cost effective, efficient and fast for the removal of dye from aqueous solutions. As a result, we consider that this study will be useful in designing biomass–TiO_2 co-sorbent system and diminishing time for sustainable dye removal and complete shortcomings of the literature.

Nomenclature

A	the solution pH
a	the number of levels
B	the initial dye concentration (mg/L)
C	the contact time (min)
C_e	the liquid phase concentrations of dye at equilibrium (mg/L)
C_0	the liquid phase concentrations of dye at initial (mg/L)
k	the number of factors
K_F	Freundlich sorption constant $(mg/g(L/mg)^{1/n})$
K_L	Langmuir constant related to rate of sorption (L/mg)
k_1	the rate constant of pseudo-first order sorption (min^{-1})

k_2	the rate constant of pseudo-second order sorption (g/mg min)
n	Freundlich heterogeneity factor
P	probability level
q_e	the amount of dye sorbed per unit weight of sorbent at equilibrium (mg/g)
$q_{e,cal}$	the calculated sorption capacity (mg/g)
$q_{e,exp}$	the experimental sorption capacity (mg/g)
q_m	Langmuir constant related to maximum sorption capacity (mg/g)
q_t	the amount of dye sorbed per unit weight of sorbent at time (mg/g)
R^2	correlation coefficient
S	the standard error of the estimate
T	Transmittance is the fraction of incident light (electromagnetic radiation) at a specified wavelength that passes through a sample (%)
t	the contact time (min)
V	the volume of dye solution (L)
W	the amount of the sorbent used (g)
X_0	the global mean
Y	the predicted response (% removal efficiency)
λ_{max}	the wavelength at which maximum absorption occurs (nm)
η	the dye removal efficiency (%)

References

Abdallah, R., Taha, S., 2012. Biosorption of methylene blue from aqueous solution by nonviable Aspergillus fumigates. Chem. Eng. J. 195–196, 69–76. http://dx.doi.org/10.1016/j.cej.2012.04.066.

Abidi, N., Errais, E., Duplay, J., Berez, A., Jrad, A., Schäfer, G., Ghazi, M., Semhi, K., Trabelsi-Ayadi, M., 2015. Treatment of dye-containing effluent by natural clay. J. Clean. Prod. 86, 432–440. http://dx.doi.org/10.1016/j.jclepro.2014.08.043.

Ahmad, M.A., Rahman, N.K., 2011. Equilibrium, kinetics and thermodynamic of Remazol Brilliant Orange 3R dye adsorption on coffee husk-based activated carbon. Chem. Eng. J. 170, 154–161. http://dx.doi.org/10.1016/j.cej.2011.03.045.

Aksu, Z., Isoglu, I.A., 2006. Use of agricultural waste sugar beet pulp for the removal of Gemazol turquoise blue-G reactive dye from aqueous solution. J. Hazard. Mater. 137, 418–430. http://dx.doi.org/10.1016/j.jhazmat.2006.02.019.

Allen, S.J., Murray, M., Brown, P., Flynn, O., 1994. Peat as an adsorbent for dyestuffs and metals in wastewater. Resour. Conserv. Recycl. 11, 25–39. http://dx.doi.org/10.1016/0921-3449(94)90076-0.

Antony, J., 2003. Design of Experiments for Engineers and Scientists. Butterworth-Heinemann, New York, ISBN 978-0-7506-4709-0.

Auta, M., Hameed, B.H., 2012. Modified mesoporous clay adsorbent for adsorption isotherm and kinetics of methylene blue. Chem. Eng. J. 198–199, 219–227. http://dx.doi.org/10.1016/j.cej.2012.05.075.

Barredo-Damas, S., Alcaina-Miranda, M.I., Iborra-Clar, M.I., Mendoza-Roca, J.A., 2012. Application of tubular ceramic ultrafiltration membranes for the treatment of integrated textile wastewaters. Chem. Eng. J. 192, 211–218. http://dx.doi.org/10.1016/j.cej.2012.03.079.

Cardoso, N.F., Pinto, R.B., Lima, E.C., Calvete, T., Amavisca, C.V., Royer, B., Cunha, M.L., Fernandes, T.H.M., Pinto, I.S., 2011. Removal of remazol black B textile dye from aqueous solution by adsorption. Desalination 269, 92–103. http://dx.doi.org/10.1016/j.desal.2010.10.047.

Depci, T., Kul, A.R., Önal, Y., 2012. Competitive adsorption of lead and zinc from aqueous solution on activated carbon prepared from Van apple pulp: study in single- and multi-solute systems. Chem. Eng. J. 200–202, 224–236. http://dx.doi.org/10.1016/j.cej.2012.06.077.

Elkady, M.F., Ibrahim, A.M., Abd El-Latif, M.M., 2011. Assessment of the adsorption kinetics, equilibrium and thermodynamic for the potential removal of reactive red dye using eggshell biocomposite beads. Desalination 278, 412–423. http://dx.doi.org/10.1016/j.desal.2011.05.063.

Farzana, M.H., Meenakshi, S., 2014. Decolorization and detoxification of acid blue 158 dye using cuttlefish bone powder as co-adsorbent via photocatalytic method. J. Water Process Eng. 2, 22–30. http://dx.doi.org/10.1016/j.jwpe.2014.03.010.

Foo, K.Y., Hameed, B.H., 2011. Preparation and characterization of activated carbon from sunflowerseed oil residue via microwave assisted K_2CO_3 activation. Bioresour. Technol. 102, 9794–9799. http://dx.doi.org/10.1016/j.biortech.2011.08.007.

Food and Agriculture Organization of the United Nations, 2014. (accessed 15.07.14.), <http://faostat.fao.org/site/567/DesktopDefault.aspx?PageID=567#ancor>.

Gupta, V.K., Jain, R., Varshney, S., 2007. Removal of reactofix golden yellow 3 RFN from aqueous solution using wheat husk—an agricultural waste. J. Hazard. Mater. 142, 443–448. http://dx.doi.org/10.1016/j.jhazmat.2006.08.048.

Jain, A.K., Gupta, V.K., Bhatnagar, A., Suhas, 2003. Utilization of industrial waste products as adsorbents for the removal of dyes. J. Hazard. Mater. 101, 31–42. http://dx.doi.org/10.1016/S0304-3894(03)00146-8.

Kaouah, F., Boumaza, S., Berrama, T., Trari, M., Bendjama, Z., 2013. Preparation and characterization of activated carbon from wild olive cores (oleaster) by H_3PO_4 for the removal of basic red 46. J. Clean. Prod. 54, 296–306. http://dx.doi.org/10.1016/j.jclepro.2013.04.038.

Kara, S., Aydiner, C., Demirbas, E., Kobya, M., Dizge, N., 2007. Modeling the effects of adsorbent dose and particle size on the adsorption of reactive textile dyes by fly ash. Desalination 212, 282–293. http://dx.doi.org/10.1016/j.desal.2006.09.022.

Kavak, D., 2009. Removal of boron from aqueous solutions by batch adsorption on calcined alunite using experimental design. J. Hazard. Mater. 163, 308–314. http://dx.doi.org/10.1016/j.jhazmat.2008.06.093.

Khorramfar, S., Mahmoodi, N.M., Arami, M., Bahrami, H., 2011. Oxidation of dyes from colored wastewater using activated carbon/hydrogen peroxide. Desalination 279, 183–189. http://dx.doi.org/10.1016/j.desal.2011.06.005.

Kokabian, B., Bonakdarpour, B., Fazel, S., 2013. The effect of salt on the performance and characteristics of a combined anaerobic–aerobic biological process for the treatment of synthetic wastewaters containing reactive black 5. Chem. Eng. J. 221, 363–372. http://dx.doi.org/10.1016/j.cej.2013.01.101.

Leechart, P., Nakbanpote, W., Thiravetyan, P., 2009. Application of waste wood-shaving bottom ash for adsorption of azo reactive dye. J. Environ. Manag. 90, 912–920. http://dx.doi.org/10.1016/j.jenvman.2008.02.005.

Liu, Y., Yang, S., Hong, J., Sun, C., 2007. Low temperature preparation and microwave photocatalytic activity study of TiO_2 mounted activated carbon. J. Hazard. Mater. 142, 208–215. http://dx.doi.org/10.1016/j.jhazmat.2006.08.020.

Mittal, A., Malviya, A., Kaur, D., Mittal, J., Kurup, L., 2007. Studies on the adsorption kinetics and isotherms for the removal and recovery of methyl Orange from wastewaters using waste materials. J. Hazard. Mater. 148, 229–240. http://dx.doi.org/10.1016/j.jhazmat.2007.02.028.

Noroozi, B., Sorial, G.A., Bahrami, H., Arami, M., 2007. Equilibrium and kinetic adsorption study of a cationic dye by a natural adsorbent—silkworm pupa. J. Hazard. Mater. 139, 167–174. http://dx.doi.org/10.1016/j.jhazmat.2006.06.021.

Özbay, N., Yargıç, A.Ş., Yarbay-Şahin, R.Z., Önal, E., 2013. Full factorial experimental design analysis of reactive dye removal by carbon adsorption. J. Chem. 1–13. http://dx.doi.org/10.1155/2013/234904.

Prasad, R.K., Srivastava, S.N., 2009. Sorption of distillery spent wash onto fly ash: kinetics, mechanism, process design and factorial design. J. Hazard. Mater. 161, 1313–1322. http://dx.doi.org/10.1016/j.jhazmat.2008.04.092.

Ramakrishna, K.R., Viraraghavan, T., 1997. Use of slag for dye removal. Waste Manag. 17, 483–488. http://dx.doi.org/10.1016/S0956-053X(97)10058-7.

Rathinam, A., Rao, J.R., Nair, B.U., 2011. Adsorption of phenol onto activated carbon from seaweed: determination of the optimal experimental parameters using factorial design. J. Taiwan Inst. Chem. Eng. 42, 952–956. http://dx.doi.org/10.1016/j.jtice.2011.04.003.

Ravichandran, P., Sowmya, A., Meenakshi, S., 2013. A comparative study on removal of basic violet 10 by adsorption and photocatalytic degradation using low cost activated carbon. Int. J. Environ. Waste Manag. 12, 189–202. http://dx.doi.org/10.1504/IJEWM.2013.055593.

Reddy, M.C.S., Sivaramakrishna, L., Reddy, A.V., 2012. The use of an agricultural waste material, jujuba seeds for the removal of anionic dye (Congo red) from aqueous medium. J. Hazard. Mater. 203–204, 118–127. http://dx.doi.org/10.1016/j.jhazmat.2011.11.083.

Safa, Y., Bhatti, H.N., 2011. Biosorption of direct red-31 and direct orange-26 dyes by rice husk: application of factorial design analysis. Chem. Eng. Res. Des. 89, 2566–2574. http://dx.doi.org/10.1016/j.cherd.2011.06.003.

Sathishkumar, P., Arulkumar, M., Palvannan, T., 2012. Utilization of agro-industrial waste Jatropha curcas pods as an activated carbon for the adsorption of reactive dye Remazol Brilliant Blue R (RBBR). J. Clean. Prod. 22, 67–75. http://dx.doi.org/10.1016/j.jclepro.2011.09.017.

Srinivasan, A., Viraraghavan, T., 2010. Oil removal from water by fungal biomass: a factorial design analysis. J. Hazard. Mater. 175, 695–702. http://dx.doi.org/10.1016/j.jhazmat.2009.10.065.

Suárez-Garcıa, F., Martınez-Alonso, A., Tascón, J.M.D., 2001. Porous texture of activated carbons prepared by phosphoric acid activation of apple pulp. Carbon 39, 1111–1115. http://dx.doi.org/10.1016/S0008-6223(01)00053-7.

Vieira, A.P., Santana, S.A.A., Bezerra, C.W.B., Silva, H.A.S., Chaves, J.A.P., de Melo, J.C.P., da Silva Filho, E.C., Airoldi, C., 2009. Kinetics and thermodynamics of textile dye adsorption from aqueous solutions using babassu coconut mesocarp. J. Hazard. Mater. 166, 1272–1278. http://dx.doi.org/10.1016/j.jhazmat.2008.12.043.

Wang, R., Cai, X., Shen, F., 2014. TiO_2 hollow microspheres with mesoporous surface: superioradsorption performance for dye removal. Appl. Surf. Sci. 305, 352–358. http://dx.doi.org/10.1016/j.apsusc.2014.03.089.

Wang, X., Hu, Z., Chen, Y., Zhao, G., Liu, Y., Wen, Z., 2009. A novel approach towards high-performance composite photocatalyst of TiO_2 deposited on activated carbon. Appl. Surf. Sci. 255, 3953–3958. http://dx.doi.org/10.1016/j.apsusc.2008.10.083.

Wei, M.C., Wang, K.S., Huang, C.L., Chiang, C.W., Chang, T.J., Lee, S.S., Chang, S.H., 2012. Improvement of textile dye removal by electrocoagulation with low-cost steel wool cathode reactor. Chem. Eng. J. 192, 37–44. http://dx.doi.org/10.1016/j.cej.2012.03.086.

Yargıç, A.Ş., Yarbay Şahin, R.Z., Özbay, N., Önal, E., 2015. Assessment of toxic copper(II) biosorption from aqueous solution by chemically-treated tomato waste (Solanum lycopersicum). J. Clean. Prod. 88, 152–159. http://dx.doi.org/10.1016/j.jclepro.2014.05.087.

Yola, M.L., Eren, T., Atar, N., Wang, Shaobin, 2014. Adsorptive and photocatalytic removal of reactive dyes by silver nanoparticle-colemanite ore waste. Chem. Eng. J. 242, 333–340. http://dx.doi.org/10.1016/j.cej.2013.12.086.

Yuan, R., Ramjaun, S.N., Wang, Z., Liu, J., 2012. Photocatalytic degradation and chlorination of azo dye in saline wastewater: kinetics and AOX formation. Chem. Eng. J. 192, 171–178. http://dx.doi.org/10.1016/j.cej.2012.03.080.

Zhou, K., Zhang, Q., Wang, B., Liu, J., Wen, P., Gui, Z., Hu, Y., 2014. The integrated utilization of typical clays in removal of organic dyes and polymer nanocomposites. J. Clean. Prod. 81, 281–289. http://dx.doi.org/10.1016/j.jclepro.2014.06.038.

Zolgharnein, J., Bagtash, M., Asanjarani, N., 2014. Hybrid central composite design approach for simultaneous optimization of removal of alizarin red S and indigo carmine dyes using cetyltrimethylammonium bromide-modified TiO_2 nanoparticles. J. Environ. Chem. Eng. 2, 988–1000. http://dx.doi.org/10.1016/j.jece.2014.03.017.